SIMULATION OF HEAT AND MASS TRANSFER IN SUNS RIVER SOLAR DISTILLATION

HOUMAN AZARI

Department of Civil Engineering

APPROVED:

W. Shane Walker, Ph.D., Chair

John Walton, Ph.D.

Ivonne Santiago, Ph.D.

Norman Love, Ph.D.

Charles Ambler, Ph.D.
Dean of the Graduate School

Dedicated

To my

Beloved *FAMILY*

SIMULATION OF HEAT AND MASS TRANSFER IN SUNS RIVER SOLAR DISTILLATION

By

HOUMAN AZARI, B.S.

THESIS

Presented to the Faculty of the Graduate School of

The University of Texas at El Paso

In Partial Fulfillment

of the Requirements

for the Degree of

MASTER OF SCIENCE

Department of Civil Engineering

THE UNIVERSITY OF TEXAS AT EL PASO

December 2014

ACKNOWLEDGEMENTS

First, I would like to thank the committee members for spending time and energy on my thesis. Their comments and suggestions were priceless for accomplishing this work. I would like to thank Dr. Love for his guidance in creating the thermal-resistance model. I wish to thank Dr. Walton for his helpful guidance about radiation heat transfer and his efforts for making my thesis more clear, especially in grammar and vocabulary. I also want to thank Dr. Santiago for her attention to my thesis; her comments helped me significantly improve my thesis.

I would like to express my deep gratitude to my advisor, Dr. Walker for his time, patience, encouragement, and support. Honestly, without his supervision and help, I could not have completed this work. Beside his academic knowledge and abilities, his encouragement helped me to overcome all my doubts.

I want to thank The University of Texas at El Paso and the Department of Civil Engineering for giving me this opportunity to study Environmental Engineering. I will be always grateful to Dr. Soheil Nazarian, the kind and dear advisor of Department of Civil engineering, for guiding me through the admission process and helping me come back to school.

I want to express my deepest respect to all my academic teachers in The University of Texas at El Paso, especially my professors in the Department of Civil Engineering.

For sure, I thank my dear wife Negin, for understanding, helping, and supporting me during my education.

And at last, I want to appreciate supports and prayers of my parents, sisters and friends.

In our culture, we have a proverb which says: “If you don’t appreciate the kindness of the others, you won’t be able to be grateful to the Lord”. Thank you, God, for loving and supporting me; anything that I have is your grace. I truly love you.

ABSTRACT

SIMULATION OF HEAT AND MASS TRANSFER IN SUNS RIVER SOLAR DISTILLATION

HOUMAN AZARI, M.S.

THE UNIVERSITY OF TEXAS AT EL PASO

December 2014

Many regions around the world have limited fresh water resources, and we need to desalinate brackish water resources for drinking and irrigation purposes. Most of the world is also facing energy challenges which encourages engineers and scientists to use renewable energy resources instead of hydrocarbon fuels. Arid regions such as the Middle East, many African countries, and the southwestern United States typically have abundant solar irradiance and brackish or saline water supplies. Solar-thermal desalination could be an important supply of fresh water in these regions.

The classic solar still is not efficient for providing large amounts of clean water for drinking and irrigation purposes. KII Inc. is a private American company that has developed a new type of solar still, called the Suns River Still (SRS), which has a solar evaporator separated from an active distillate condenser. The latest prototype was tested by KII Inc. at the Brackish Groundwater National Desalination Research Facility (BGNDRF) in Alamogordo, NM.

The goal of this thesis research was to analyze the performance of the SRS to identify opportunities to further improve the performance of the still. The energy efficiency of the still was observed to be 83%, and analysis of heat losses revealed that 86% of losses were due to radiation from the solar window. Use of low-emissivity glass would significantly decrease heat loss, but may not be worthwhile due to a lower transmissivity and decreased capture of solar energy.

TABLE OF CONTENTS

LIST OF FIGURES

LIST OF TABLES

1 INTRODUCTION

1.1 Desalination Background

The need for safe, clean drinking water is increasing growing. Rapid economic growth and awareness of climate change have resulted in increasing pressure to develop water resources of reliable quality and quantity, especially in arid and developing countries. Sometimes, sufficient water quantity is available, but the water is brackish or saline and must be desalinated to make it safe to drink. There are two major ways to desalinate brackish and saline water: thermal processes and membrane processes. Arid regions such as the Middle East, many African countries, and the southwestern United States typically have abundant solar irradiance and brackish or saline water supplies. The main goal of this research is to improve water access to families and small communities in arid and developing regions by improving solar-thermal desalination technology to take advantage of brackish and saline water supplies and abundantly available solar power.

1.2 Solar Distillation

Distillation is a process of separating the substances from a liquid mixture by evaporating and condensing (Encyclopedia Britannica 2014). Distillation of brackish or saline water typically produces a distillate product with very low total dissolved solids.

A solar still uses the heat of the sun to drive evaporation (Ranjan and Kaushik 2013). Solar stills have been used for centuries to produce potable water, particularly in remote arid areas and out on the sea. Solar stills typically produce less drinking water per unit volume than fuel-based desalination processes, but solar stills have the advantage of utilizing a renewable energy source. The majority of solar stills are small scale, and they are typically designed to be economically feasible rather than optimized for distilling potential.

1.2.1 Classic Solar Still Distillation

The basic principles of solar water distillation are simple, and it works as the way nature makes rain. Heat from the sun evaporates water, and the water vapor rises until it condenses on the transparent surface, as shown in Figure 1. The condensate (distillate) flows down to the collector. This process removes impurities, such as salts and heavy metals, and eliminates microbiological organisms.

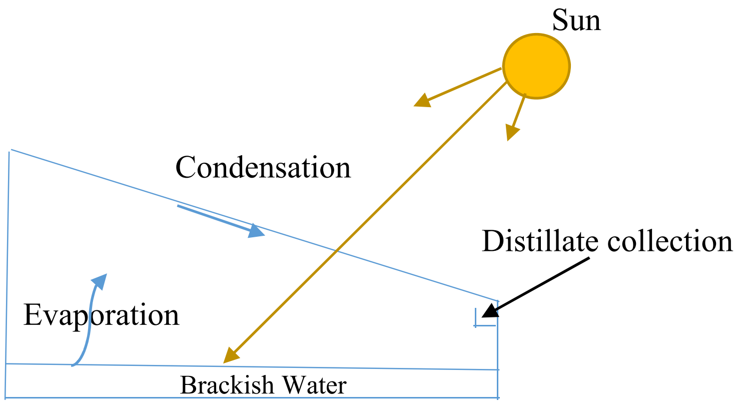

Figure 1 – Conceptual diagram of a classic solar still

In the classic type of stills, the rate of evaporation of the water and its convection to the top of the still is relatively slow, and greater water depth may reduce the rate of evaporation. Furthermore, the condensation of water vapor on the top of the still blocks light from entering. A classic solar still produces around 3 L/m^2/day with an efficiency of about 30% (Ranjan and Kaushik 2013).

1.2.2 Suns River Still (SRS)

Today, the world economy steadily shifts from a hydrocarbon basis to more natural and sustainable energy-based forms (Ahuja *et al*., 2009). In the field of desalination, there is an interest in developing solar still devices into a more efficient technology for sustainable water production. So, increasing the productivity of solar stills has been the focus of intensive research.

Hill Kemp is the owner of a private company in the U.S.A called KII Inc., and he has invented a new type of solar still called the Suns River Still (SRS). The SRS desalination process is patented in the USA (Patent #8,088,257 and #8,580,085) and in Australia (Patent #2008317021). The SRS is an improvement over the classic solar still (KII Inc., 2014).

The SRS has a double-paned glass-topped box held an angle to allow sunlight inside to evaporate water in the top section, with a condenser section underneath the evaporator, as shown in Figure 2. In the evaporator, a thin-film waterfall of brackish water cascades down the inclined evaporator pan and is heated by the incident light; the brackish water at the bottom of the evaporator pan is recirculated to the top of the pan. Water is vaporized from the brackish surface recirculation, and the warm-humid air rises by natural convection to the top of the still. In the condenser, under the evaporator pan, a coiled plastic tube carries a counter-current flow of relatively cool brackish water to provide a condensing surface. Water is condensed out of the humid air as it travels down the condenser, and relatively dry air is supplied to the bottom of the evaporator. Warm brackish water exiting the condenser coil is transferred to a 2nd effect, which is simply a classic greenhouse canopy solar still with a pool of brackish water.

The walls of the SRS are constructed with steel and insulation foam to minimize heat loss by conduction, and the evaporator pan is made of stainless steel with insulation foam underneath to minimize heat transfer from the evaporator to the condenser. The evaporator pan surface is covered with black fabric to maintain the water film and provide a relatively high absorptivity of incident thermal radiation.

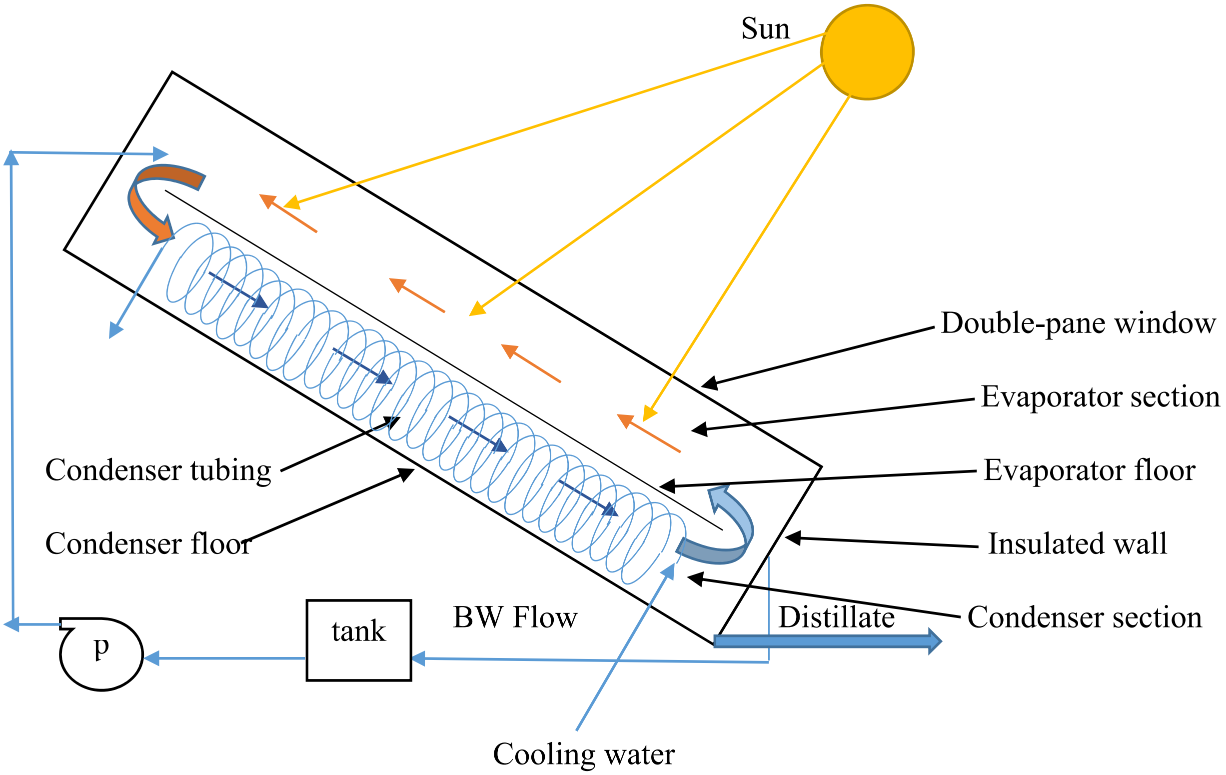

Figure 2 – Conceptual diagram of the Suns River Still

1.3 Goals and Objectives

The goal of this research is to improve the effectiveness and efficiency of the Suns River Still (SRS). To support this goal, the objectives of this research were to: (1) analyze the thermal efficiency of the SRS; (2) simulate heat losses through the still envelope and analyze insulation efficiency; and (3) analyze the performance of the still with respect to potential optimization.

2 METHODOLOGY

2.1 Suns River Still (SRS) Experimentation at BGNDRF

The prototype SRS was tested at the Brackish Groundwater National Research and Development Facility (BGNDRF) at Alamogordo, New Mexico. BGNDRF has multiple brackish groundwater wells and multiple test bays to support the testing of desalination technology (U.S. Bureau of Reclamation 2014).

KII Inc. began testing the original prototype at BGNDRF in the spring of 2012 and has been collaborating with the UTEP Center for Inland Desalination Systems team since then. The team has made several technical improvements and fabricated subsequent prototypes. The current SRS prototype is approximately 1.0 m wide and 2.7 m long and is mounted at a 30° incline. A side view of the SRS is shown in Figure 3 and a front view of the SRS is shown in Figure 4.

Figure 3 – The SRS: side view

Figure 4 – The SRS: front view

Data collected by KII Inc. from the SRS at BGNDRF on August 28, 2014 included solar irradiance and distillate volume (Figure 5), and several temperatures within the still (Figure 6) throughout the day. Solar irradiance was measured with a hand-held pyranometer; distillate volume was measured using graduated cylinders; and temperatures were measured with thermocouples.

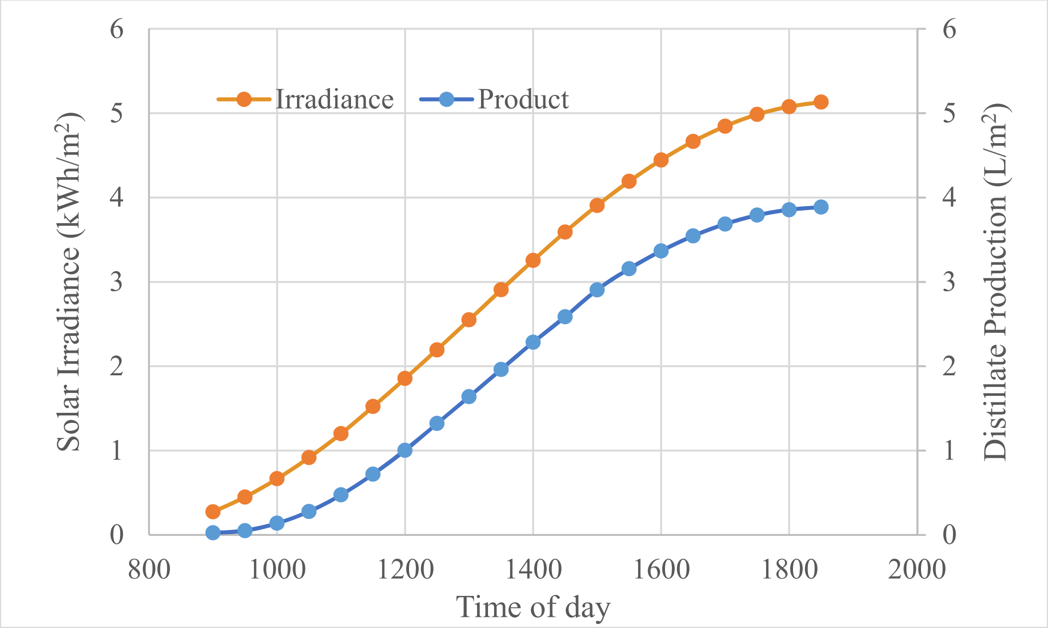

Figure 5 – BGNDRF solar irradiance and SRS distillate volume for August 28, 2014

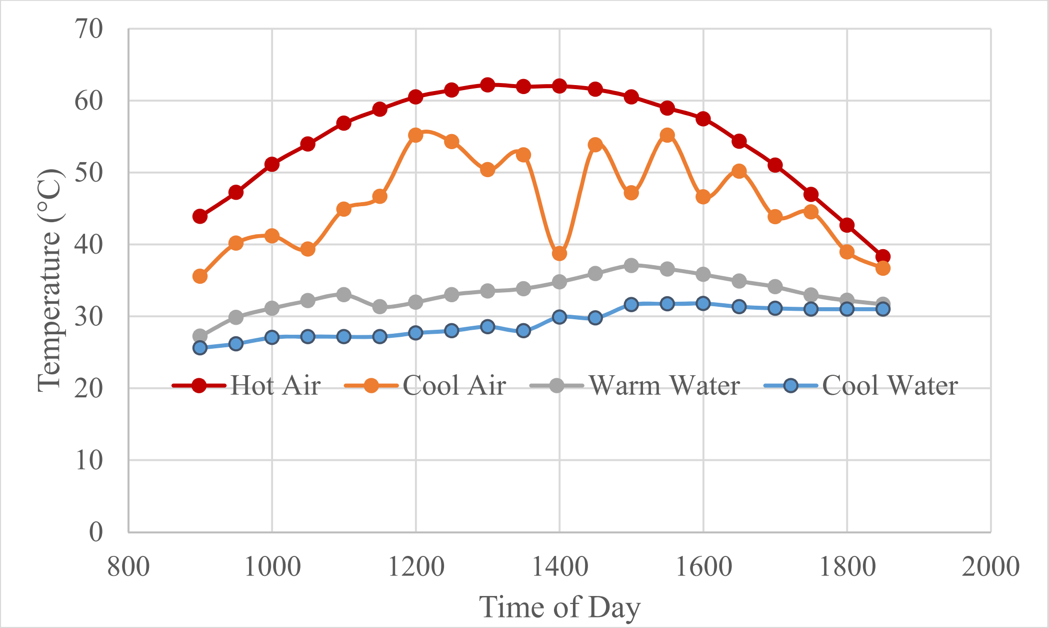

Figure 6 – SRS operational temperatures for August 28, 2014

2.2 Analysis of Energy Efficiency of SRS

The thermal efficiency (η) is a dimensionless performance measure of a device with respect to thermodynamics. For every device that uses thermal energy, the thermal efficiency is the ratio of the useful output of energy from a device compared to its input (Cengel *et al*., 2002):

Equation 1 $$\eta = Q_{out}/Q_{in}$$

And:

Equation 2 $$Q_{in} = \tau \, Q_{solar}$$

Where:

τ = Transmissivity of glass (dimensionless)

For SRS, the solar radiance is our input energy (Q_{in}), and the output energy is the cumulative increase in enthalpy of the water leaving the condenser coil. By measuring the input and output temperature of cooling water, we calculated the output energy with the equation:

Equation 3 $$\dot{Q}_{out} = \dot{m} c \Delta T$$

Where:

$\dot{Q}$ = Heat transfer rate [kW]

$\dot{m}$ = Mass rate of water through the condenser coil [kg/s]

c = Specific heat of water [kJ/kg.K]

ΔT = Temperature difference [K]

And:

Equation 4 $$Q_{out} = \dot{Q}_{out} \, t$$

Where:

t = Time [s] (the model time step of 3600 s)

2.3 Simulating heat losses through the SRS envelope

2.3.1 Thermal resistance model for conduction and convection

Microsoft Excel was used to create a thermal resistance model of heat loss by conduction and convection through the envelope of the SRS (Cengel *et al* 2012). First, dimensions and materials data were collected from KII Inc. Second, reference values of thermal properties of the materials were collected. Then, a thermal resistance model was developed using the following equations.

Convection resistance was calculated as:

Equation 5

$$\mathbf{R_{conv}} = \frac{\mathbf{1}}{\mathbf{hA}}$$

where:

R_{conv} = Convection resistance [K/W]

h = Convection heat transfer coefficient [W/m^2.K]

A = Surface area [m^2]

Conduction resistance was calculated as:

Equation 6

$$\boldsymbol{R_{cond} = L/kA}$$

Where:

R_{cond} = Conduction resistance [K/W]

L = Material thickness [m]

k = Thermal conductivity [W/m.K]

A = Surface area [m^2]

The amount of heat flow is calculated by:

Equation 7

$$\boldsymbol{Q = \Delta T/\Sigma R}$$

Where:

$\dot{Q}$ = Heat Transfer Rate [W]

ΔT = Temperature Difference [K]

In the evaporator, energy is lost from the still through the double-pane window and the walls. Thus, the following thermal resistances were modeled in series for walls, as illustrated in Figure 7. This is a conceptual cross-section of the insulated walls in Figure 2.

- Interior natural convection (R_1).
- Interior steel wall conduction (R_2).
- Internal wall insulation conduction (R_3).
- Exterior steel wall conduction (R_4).
- Exterior forced convection-wind (R_5).

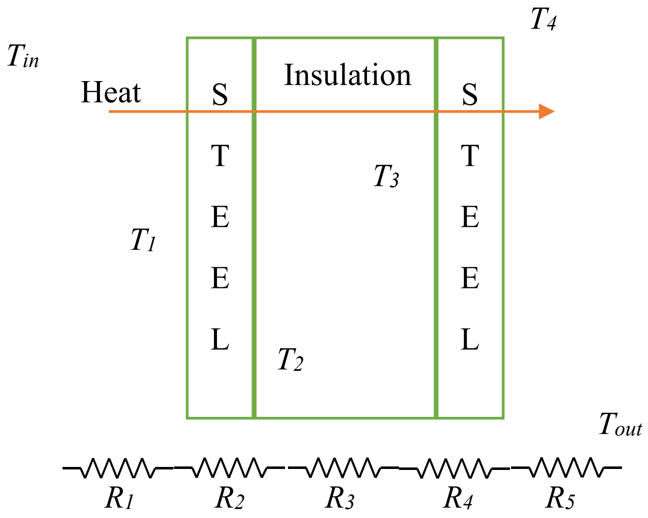

Figure 7 – Thermal-resistance model for cross-section of the SRS walls

For the double-pane window, these resistances were considered, as shown in Figure 8:

- Exterior forced convection-wind (R_1).
- Exterior glass conduction (R_2).
- Internal air gap convection (R_3) in parallel with R_4
- Internal air gap conduction (R_4) in parallel with R_3
- Interior glass conduction (R_5).
- Interior natural convection (R_6).

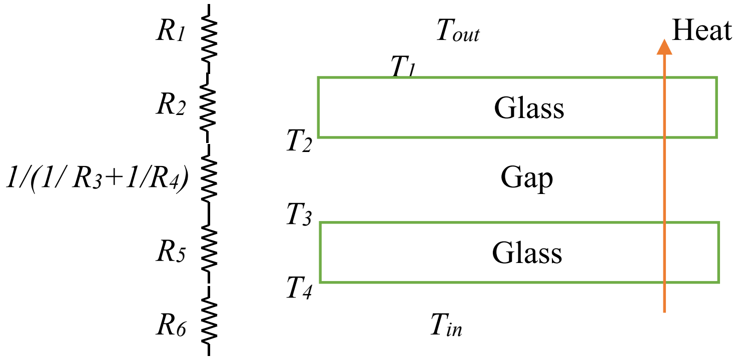

Figure 8 – Thermal-resistance model for cross-section of double-pane window

The condenser loses heat from the still through the condenser walls and the condenser floor. For the walls, the thermal resistances considered are the same as the evaporator walls shown in Figure 7. For the condenser bed, the following resistances were considered:

- Interior natural convection (R_1).
- Water film convection (R_2) in parallel with R_3.
- Water film conduction (R_3) in parallel with R_2.
- Interior steel surface conduction (R_4).
- Internal insulation conduction (R_5).
- Exterior steel conduction (R_6).
- Exterior forced convection-wind (R_7).

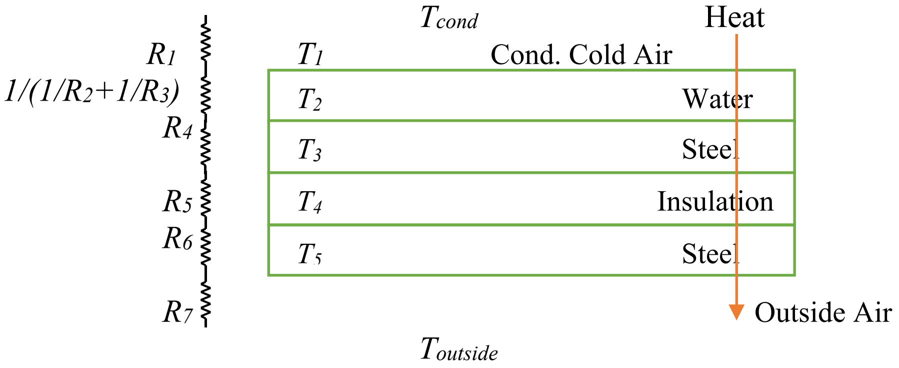

Figure 9 – Thermal-resistance model for cross-section of condenser floor

2.3.2 Calculation of heat transfer coefficients

Since the h value is variable in different conditions (*e.g.* temperature and speed), we calculated h separately for each case (Cengel *et al*., 2002). Wind around the outside of the still was simulated as forced-convection according to the following equations:

Equation 8 $$Re = LV/v$$

Equation 9 $$Nu = 0.037\,(Re^{0.8}-871)\,Pr^{1/3}$$

Equation 10 $$h = kNu/L$$

With:

Re = Reynolds number (dimensionless)

Nu = Nusselt number (dimensionless)

Pr = Prandtl number of air at film temperature (dimensionless)

k = Thermal conductivity of air at film temperature [W/m.K]

v = Kinematic viscosity of air at film temperature [m^2/s]

L = The length of solar still [m]

For water film on the evaporator floor, as well as air recirculation within the evaporator and condenser, convection was calculated as:

Equation 11 $$Ra = Cos\theta g\,\beta\Delta TL^3Pr/v^2$$

Equation 12 $$Nu = 0.1Ra^{1/3}$$

Equation 13 $$h = kNu/L$$

With:

Ra = Raleigh number (dimensionless)

θ = The angle of solar still

β = The coefficient of volume expansion [1/K]

L = The length of solar still [m]

2.3.3 Modeling of radiation

Heat losses were calculated due to thermal radiation (emission) from the following external surfaces:

- Evaporator window
- Evaporator walls
- Condenser walls
- Condenser floor

Heat flow by radiation was calculated by:

Equation 14 $$Q = \varepsilon\sigma A[T_{surface}^4 - (T_{ambient} - \Delta T_{sky})^4]$$

Where:

ε = Emissivity (dimensionless)

$\sigma = 5.67 \cdot 10^{-8}$ [W/m².K^4] (Stefan-Boltzmann Constant)

A = Surface area [m²]

T = Temperature [K]

ΔT_{sky} = Relative temperature difference between ambient air and the sky [K]

Madeira *et al* (2002) modeled the radiation losses to the sky based on a relative temperature difference between the ambient air and the sky of: 20 K for cloudless skies, 15 K for high altitude cloudy skies, and 10 K for low altitude cloudy skies. For the model developed for the SRS, the temperature difference of 8 K was observed to close the heat balance for Aug 28:

Equation 15 $$0 = Q_{solar} - Q_{loss} - Q_{condens}$$

Where:

Q_{solar} = Total daily solar irradiance [kWh]

Q_{loss} = Total heat loss [kWh]

$Q_{condens}$ = Total outgoing energy from condenser tubing [kWh]

2.4 Simulating heat transfer through the condenser coil

The condenser operates like a shell-and-tube heat exchanger with a cross-linked polyethylene (PEX) tubing that is coiled inside the condenser. Unlike minimizing heat transfer through the envelope of the still, the condenser tubing heat transfer should be maximized. The thermal resistances considered for the condenser tubing are the following, as shown in Figure 10:

- Interior forced convection-brackish water (R_1).
- Tubing wall conduction (R_2).
- Exterior convection-condensation (R_3).

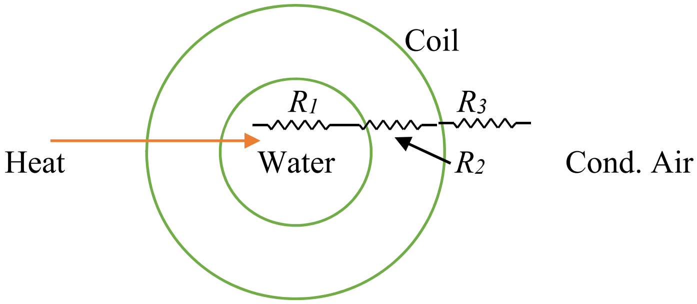

Figure 10 – Thermal-resistance model for cross-section of condenser tubing

For the cooling water flowing inside the condenser tubing, convection was modeled as:

Equation 16 $$Re = DV/v$$

Equation 17 $$Nu = 0.023Re^{0.8}Pr^{0.4}$$

Equation 18 $$h = kNu/D$$

Where:

D = External diameter of coil [m]

For saturated air flowing around the condenser tubing, convection around the outside of the condenser tubing was modeled as:

Equation 19 $$Re = DV/v$$

Equation 20 $$Nu = 0.683Re^{0.466}Pr^{1/3}$$

Equation 21 $$h = kNu/D$$

With:

V = Saturated air speed [m/s]

The overall heat transfer coefficient (U) of the tubing was estimated as:

Equation 22 $$U = 1/(\Sigma R_{coil}A)$$

Where:

U = Overall heat transfer coefficient of tubing [W/m².K]

ΣR_{coil} = Resistance summation for tubing [K/W]

A = Outside area of tubing [m²]

The U-value was also calculated using the Log Mean Temperature Difference (LMTD) of the data on August 28, 2014:

Equation 23 $$\Delta T_{lm} = ((T_{air\text{-}in}-T_{tube\text{-}out}) - (T_{air\text{-}out}-T_{tube\text{-}in})) / \ln((T_{air\text{-}in}-T_{tube\text{-}out})/(T_{air\text{-}out}-T_{tube\text{-}in}))$$

And:

Equation 24 $$\dot{Q} = UA\Delta T_{lm}$$

Where:

$\dot{Q}$ = mcΔT (Equation 3)

2.5 Simulating mass transfer in the condenser

The maximum distillate mass of water vapor transferred to liquid water on the condenser tubing was calculated based on the average enthalpy of vaporization of water and the :

Equation 25 $$h_{fg} = 2500.9 \text{ kJ/kg} - (2.38 \text{ kJ/kg°C})\, T$$

With:

h_{fg} = Enthalpy of vaporization [kJ/kg]

T = Temperature of the condensing water [°C]

Using Equation 3, the average heat flow can be calculated for each hour and used to estimate the hourly mass of distillate:

Equation 26 $$m_{distillate} = \dot{Q}\, t / h_{fg}$$

With:

$m_{distillate}$ = The amount of distillate [kg]

t = Time step [s] (*e.g.*, 3600 s)

3 RESULTS AND DISCUSSION

3.1 Overall Efficiencies

For the Suns River Still (SRS) performance at BGNDRF on August 28, 2014, the enthalpy gain of the brackish cooling water was calculated as 10.8 kWh, and the total solar irradiance (accounting for the transmissivity of the glass) was 13.0 kWh (4.62 kWh/m^2), which yields a thermal efficiency of 83% as shown in Figure 11.

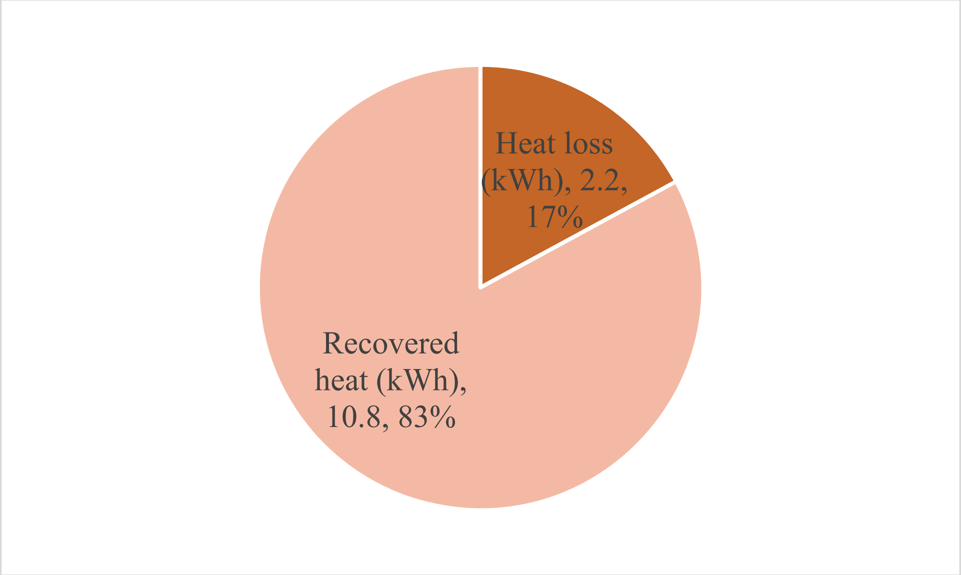

Figure 11 – Recovered latent heat and heat losses

The actual mass of distillate produced by the SRS at BGNDRF on August 28, 2014 was 10.92 kg, but the maximum mass of distillate that could have been produced by the heat recovered in the effluent cooling water was 16.3 kg. Thus, the latent heat of vaporization of the distillate produced represents 67% of the total recovered heat (10.8 kWh of enthalpy gain) in the cooling water.

3.2 Simulation of Heat Losses

The convection and conduction heat transfer resistance through the evaporator section of SRS was simulated using the precise dimensions and material properties of the SRS. (These data for dimensions and materials are proprietary and not included in this thesis.)

Thermal resistances details for the evaporator walls are shown in Table 1. The insulation provides 72% of the thermal resistance of the wall, and the exterior convection provides negligible thermal resistance.

Table 1 – Thermal resistances for evaporator wall

Resistance in Figure 7 – Thermal-resistance model for cross-section of the SRS walls	Layer	Resistance (K/W)
R1	interior convection	1.92
R2	interior wall conduction	0.00
R3	insulation conduction	4.94
R4	exterior wall conduction	0.00
R5	exterior convection	0.04
	Total wall	6.90

Thermal resistances through the window are shown in Table 2. The glass provides a very low thermal resistance, and most of the thermal resistance was estimated to occur in the convection on the internal surface.

Table 2 – Thermal resistances for double-pane window

Resistance in Figure 8	Layer	Resistance (K/W)
R1	exterior convection	0.040
R2	glass conduction	0.003
R3	gap conduction (0.165)	0.107
R4	gap convection (0.306)	
R5	glass conduction	0.003
R6	interior convection	0.306
	Total window	0.463

For the condenser floor, the thermal resistances are shown in Table 3. The insulation layer provides 87% of the thermal resistance in the condenser floor.

Table 3 – Thermal resistances for condenser floor

Resistance in Figure 9	Layer	Resistance (K/W)
R1	interior convection	0.19
R2	water film convection (0.00)	0.00
R3	water film conduction (0.00)	
R4	interior floor conduction	0.00
R5	insulation conduction	1.58
R6	exterior floor conduction	0.00
R7	exterior convection	0.04
	Total floor	1.81

Thermal resistances of the condenser wall layers are shown in Table 4. The insulation layer provides 80% of the thermal resistance in the condenser wall cross section.

Table 4 – Thermal resistances for condenser wall

Resistance in Figure 7 – Thermal-resistance model for cross-section of the SRS walls	Layer	Resistance (K/W)
R1	interior convection	1.14
R2	interior wall conduction	0.00
R3	insulation conduction	4.62
R4	exterior wall conduction	0.00
R5	exterior convection	0.04
	Total wall	5.81

Based on the dimensions and material properties, consideration of heat flow resistances due to conduction and convection revealed that the evaporator window had the least thermal resistance. The sensitivity to ambient wind speed was mild. With wind speed greater than 2 m/s (4.4 mph), the affect of wind convection thermal resistance is almost constant (not shown).

Based on the average hourly temperatures for August 28, 2014, average hourly heat losses were simulated for conduction and convection (con) and radiation (rad), as shown in Table 5. When considering all heat losses (conduction, convection, and radiation), the large majority of heat loss is from the evaporator window, as shown in Figure 12.

Table 5 – Hourly heat losses for August 28, 2014

	Evaporator				Condenser			
	Window		Wall		Wall		Floor	
Hour	con. (kJ)	rad. (kJ)	con. (kJ)	rad. (kJ)	con. (kJ)	rad. (kJ)	con. (kJ)	rad. (kJ)
7	2	401	0	21	1	22	3	1
8	10	416	1	22	0	22	1	0
9	13	442	2	23	1	23	2	1
10	51	482	6	25	6	25	22	8
11	71	559	9	28	9	29	33	19
12	81	553	10	28	11	28	38	17
13	79	561	10	29	10	29	37	16
14	51	484	6	25	6	25	21	3
15	65	483	8	25	8	25	28	3
16	56	477	7	25	7	25	24	2
17	55	486	7	25	7	25	23	5
18	44	498	5	26	5	26	18	8
19	10	468	1	25	0	24	1	1
sum	588	6309	72	329	71	329	252	84
sum	6869		401		400		336	
fraction	86%		5%		5%		4%	

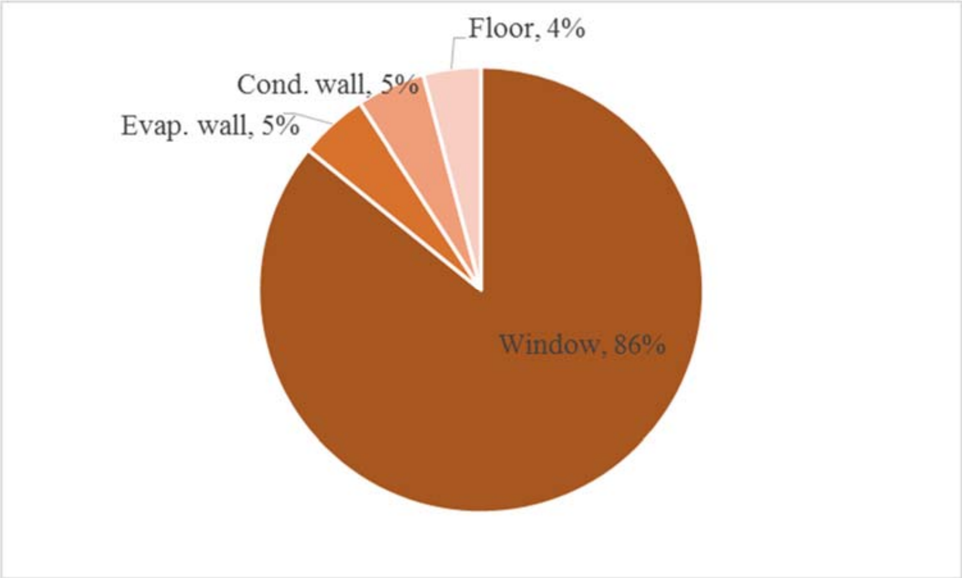

Figure 12 – Relative heat losses from the Suns River Still for Aug 28, 2014

The most significant reduction in heat loss would be accomplished by using low-emissivity glass. And to a much lesser extent, heat transfer by conduction and convection through the window could be lessened by using vacuum instead of air in the gap between the panes.

3.3 Optimization

3.3.1 Increasing the operating temperature of the evaporator

In order to increase the volume of distillate produced from the SRS, energy losses must be minimized, which will allow an increase in the operating temperature of the still. (Also, the vapor pressure of water increases nonlinearly with temperature, which could improve condensation.) To take advantage of the heat in the effluent cooling water, multiple Suns River Stills could be arranged in series to produce a hotter effluent cooling water. However, this increased operating temperature would result in increased heat losses.

Thus, five Suns River Stills were modeled in series (to a first approximation). That is, the outgoing cooling water from the first-stage SRS was simulated as feed to the second SRS condenser tubing and so forth through the fifth-stage. At the peak temperature during the day, the highest temperature was simulated as 21.6°C greater than the SRS on August 28, 2014. The corresponding simulated total heat loss in the fifth stage SRS was 25% (1946 kJ) greater than the simulated heat loss for August 28, 2014, as shown in Table 6.

Table 6 – Heat losses from elevated SRS operating temperature

	Evaporator				Condenser			
	Window		Wall		Wall		Floor	
Stage	con. (kJ)	rad. (kJ)	con. (kJ)	rad. (kJ)	con. (kJ)	rad. (kJ)	con. (kJ)	rad. (kJ)
1st SRS	588	6309	72	329	71	329	252	84
5th SRS	1250	6919	152	354	166	359	592	188
Difference	662	610	80	25	95	30	340	104
Sum	1272		105		125		444	

The velocity of air recirculating inside the solar still by natural convection also presents an opportunity for optimization as excessive air flow uses the solar energy to heat air instead of vaporizing water. With elevated operating temperatures, it may be helpful to use a valve or baffles for controlling the air velocity whenever the velocity is too high.

3.3.2 Low-emissivity glass for the evaporator

Two types of glass were compared: a plain glass with emissivity of 0.9 and transmissivity of 0.9 (used in the simulations in §3.2) and a low emissivity glass with an emissivity of 0.04 and a transmissivity of 0.8. The low emissivity glass significantly reduces the relative losses due to radiation from the window, as shown in Figure 13 (compared to Figure 12). However, the lower transmissivity of the low emissivity glass decreases the captured solar energy so that the resulting net energy gain would only be 1.8% (840 kJ) of the solar energy captured by the plain glass, as shown in Table 7. This marginal improvement may not be justifiable considering the relatively high cost of low emissivity glass.

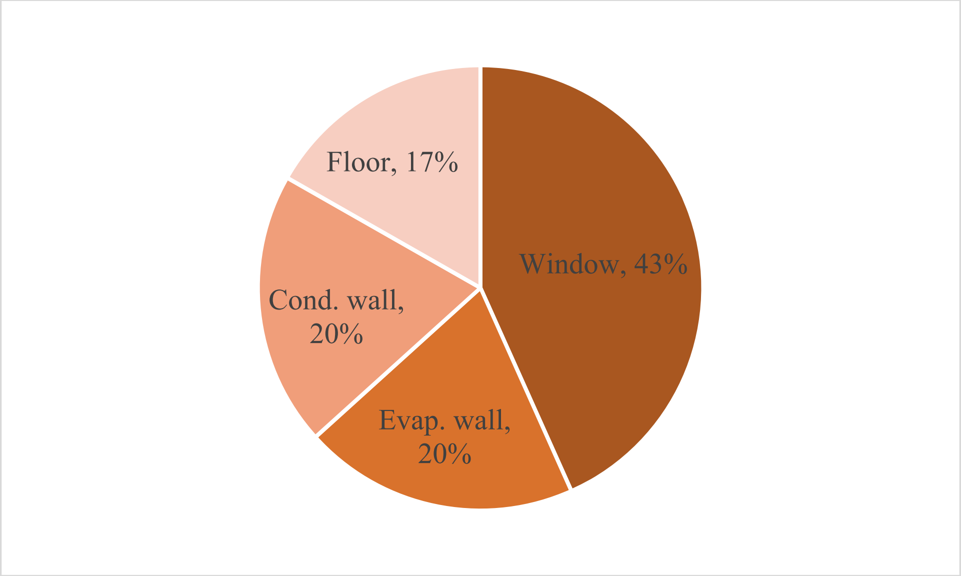

Figure 13 - Relative heat losses from the Suns River Still with low emissivity glass

Table 7 – Heat balance for two types of glasses

Glass type	E_{solar} (kJ)	E_{loss} (kJ)	E_{net} (kJ)
Plain	46691	8033	38685
Low-e	41503	2005	39485
Difference	5188	6028	840
Fraction	11.1%	12.9%	1.8%

3.3.3 Condenser tubing

The thermal resistance of the air convection around the condenser tubing is the main limitation to heat transfer, as shown in Table 8. The *U*-value of the PEX tubing was calculated based on the heat transfer resistance (Equation 22) as 18 $W/m^2.K$, and the *U*-value determined by log-mean temperature difference and heat flow (Equation 24) was approximately 27 $W/m^2.K$. For comparison, representative values of overall heat transfer coefficients for water-to-air in finned tubes are 30-60 $W/m^2.K$ (Cengel *et al* 2012).

Table 8 – Thermal resistance for condenser tubing

Resistance in Figure 10	Layer	Resistance (K/W)
R1	inside convection	0.000
R2	tubing conduction	0.002
R3	outside convection	0.016
	Total tubing	0.018

PEX has a relatively low thermal conductivity, and perhaps another inexpensive material could be identified that has a higher thermal conductivity. However, the main heat transfer resistance is actually the air convection around the tubing. So, the PEX tubing coils could be replaced with a finned surface, such as an aluminum radiator, which has a relatively high surface area and thermal conductivity with a relatively low weight. (The metal would need to be coated to avoid corrosion.) Ultimately, the cost efficiency of a finned surface would be compared to the existing PEX based on its relative price per unit area of condenser surface.

4 CONCLUSIONS

4.1 Summary

Renewable-energy-based desalination technologies are growing as solutions to fresh water shortages. In environments with abundant sunlight, solar distillation has great potential for brackish and saline water desalination. With a properly designed solar still, a family or small community could be provided with adequate amounts of clean water daily.

The existing Suns River Still (SRS) prototype is an improvement over the classic solar still with respect to specific distillate product and energy efficiency. The goal of this thesis research was to analyze the performance of the SRS to identify opportunities to improve the performance of the still.

A thermal resistance model was created to simulate the heat losses from the still based on data collected on August 28, 2014. The energy efficiency of the still was observed to be 83%, and analysis of heat losses revealed that 86% of losses were due to radiation from the solar window.

4.2 Recommendations

Based on the heat transfer modeling of the SRS, the following items are suggested for improving the system.

- Use multiple SRS units in series to increase the usefulness of the outlet hot water.
- Identify or develop a low-emissivity, high-transmissivity glass for the evaporator.
- Using a vacuum in the double-pane window gap can significantly decrease the conduction and convection heat transfer.
- Use a finned surface or radiator for improving condensation.

4.3 Future Work

Performance data with higher resolution would support more precise modeling of the SRS performance. Collecting data for the model should be a first priority, and data should be collected every 6 minutes for 24 hours, starting at 6 am and ending at 6 am the next day.

The required data are:

- Solar irradiance
- Ambient air temperature, wind speed, and visibility
- Evaporator air temperature and relative humidity (top, midpoint, and bottom)
- Evaporator brackish water temperature (top and bottom)
- Flow rate of brackish water recirculation (waterfall)
- Condenser air temperature and relative humidity (top, midpoint, and bottom)
- Inside air velocity for evaporator and condenser at the midpoint
- Feed and outlet temperature of condenser cooling water
- Flow rate of condenser cooling water

These data could be collected with sensors connected to a data acquisition system, and such data would be very useful for more detailed optimizations of components of the SRS.

REFERENCES

Ahuja, D., and Tatsutani M. (2009). “Sustainable energy for developing countries”, *Sapiens*. Vol 2, No. 1. http://sapiens.revues.org/823, Accessed December 11, 2014.

BuildingGreen.com (2012), “Energy Solutions”. http://www2.buildinggreen.com/blogs/window-performance-magic-low-e-coatings, Accessed December 14, 2014.

Cengel, Y. A. and Boles M. A. (2002). Thermodynamics, an Engineering Approach, Fourth Edition, McGraw-Hill, NY.

Cengel, Y. A., Cimbala J. M., and Turner R. H. (2012). Fundamentals of Thermal-Fluid Sciences, Fourth Edition, McGraw-Hill, NY.

Encyclopedia Britannica (2014). “Distillation.” http://www.britannica.com/EBchecked/topic/166098/distillation, Accessed December 11, 2014.

KII Inc. (2014). “Suns River Solar Still.” http://suns-river.com, Accessed November 24, 2014.

Madeira, A. C., Kim K. S., Taylor S. E., and Gleason M. L. (2002). A simple cloud-based energy balance model to estimate dew. *Agricultural and Forest Meteorology*. 111, 55-63

Ranjan, K.R. and Kaushik S.C. (2013). “Economic feasibility evaluation of solar distillation systems based on the equivalent cost of environmental degradation and high-grade energy savings” *International Journal of Low-Carbon Technologies*. http://ijlct.oxfordjournals.org/content/early/2013/06/24/ijlct.ctt048.full

U.S. Bureau of Reclamation (2014). “Brackish Groundwater National Desalination Research Facility. “http://www.usbr.gov/research/AWT/BGNDRF/history.html” , Accessed November 24, 2014.

Wikipedia (2014). “Solar Still” http://en.wikipedia.org/wiki/Solar_still, Accessed November 24, 2014.

CURRICULUM VITA

Houman Azari was born on February 10, 1971 in Tehran, Iran. The only son and second child of Aziz Azari and Heshmat Nickmanesh. He graduated from Andisheh High School, Tehran, Iran in June 1989 and entered the Sharif University of Technology in September 1989. After receiving his bachelors` of science degree in chemical/process engineering, he joined the military service on September 1994 for two years. After being discharged from military service he worked in several companies as part time jobs. He worked for Polodej construction consultant from March 2002 to September 2012. He participated in the Shiraz Combined Cycle Power Plant construction project as an EHS engineer, and he was the project engineer for the Shirvan Combined Cycle Power Plant and Rasht Hospital construction projects.

In September 2013 he entered Graduate School at The University of Texas at El Paso.

Email address: hazari2@miners.utep.edu